

Dedicated to Prof. Dorin N. Poenaru's  
70th Anniversary

# LATERAL CHARGED PARTICLE DISTRIBUTION OF EXTENSIVE AIR SHOWERS – SOURCE OF INFORMATION ABOUT ENERGY AND NATURE OF THE PRIMARY COSMIC PARTICLES

I.M. BRANCUS

National Institute for Nuclear Physics and Engineering  
P.O. Box MG-6, RO-077125 Bucharest-Magurele, Romania

(Received February 16, 2007)

*Abstract.* The CORSIKA simulated showers for H, C and Fe cosmic primaries in 8 energy intervals from  $10^{16}$  eV to  $10^{18}$  eV, taking into account the response of KASCADE-Grande detectors, have been used to reconstruct the charged particle density for KASCADE-Grande observations, based on the Linsley lateral distribution function (LDF). Extensive studies have been done to investigate features for energy estimation and mass discrimination of cosmic primaries around  $10^{17}$  eV. It has been found that the charged particle density distribution of EAS exhibits interesting information for both aspects: at larger distances from shower core, around 500 m – 600 m the charge particle density could be used as energy identifier, and at shorter distances from shower core, around, 100 m – 200 m, it signals the mass of the EAS primary.

*Key words:* cosmic rays, extensive air showers, charged particles.

## 1. INTRODUCTION

When addressing the still, in general, unsolved problems about the origin, the acceleration mechanisms and the propagation of primary cosmic rays, we have only few observable quantities at disposal for the experimental basis of far-reaching theoretical approaches and conjectures: the *energy spectrum* of the primary cosmic particles, impinging our Earth's atmosphere, the energy variation of the *chemical (mass) composition* and at sufficiently high energies

– where the influence of galactic and intergalactic fields have less influence on the paths of the charged particles – the *arrival time directions* of the primaries.

Due to the steeply falling primary energy spectrum, above  $10^{14} - 10^{15}$  eV these quantities elude from the *direct* observation by balloon or satellite borne experiments, since not yet accessible large exposure times and sensitive areas of the detectors would be needed. Fortunately there develops a phenomenon called Extended Air Shower (EAS) by the cascading interactions of the primary cosmic particle with the nuclei of the Earth's atmosphere, effectively multiplying the single particle of high energy from the outer space into a large number of charged particles (electrons and muons) of detectable energies, which arrive at the ground, distributed over a larger area around the original direction of the primary particle (shower axis). This lateral distribution carries some information about the energy and the mass of the primary particles.

This paper compiles some results [1–8] of studies of that information performed in context of the KASCADE-Grande experiment [9] for EAS observations in the energy range of  $10^{16} - 10^{18}$  eV.

The cosmic ray experiment KASCADE-Grande, set up in Forschungszentrum Karlsruhe, Germany as a multi-detector installation, investigates the electromagnetic and the muonic EAS components for each observed shower event by an array of scintillation detectors. The present results are based on simulations, using the Monte Carlo simulation program CORSIKA [10] which does not take into account the distortions by the apparatus for the experimental observations. Thus for a useful prediction of the lateral distributions and derived quantities, significant for an estimate of energy and mass, the detector response and the efficiency of the detection and reconstruction have been included, since the true density  $\rho_{\text{ch}}(r)$  (as simulated by CORSIKA) differs from the measured one  $S(r)$ .

The investigation of the energy estimate is largely inspired by the studies of Hillas [11] who has demonstrated that the charged particle density  $S^{500}$ , measured at  $r = 500$  m distance from the shower axis is a rather good estimator for the primary energy of about  $10^{17}$  eV. Here the fluctuation of the density are minimized and the value of the density proves to be mass-independent. The AGASA experiment [12, 13], covering a larger energy range, found the use of  $S^{600}$  preferable.

In our studies we found that the region around 100 – 200 m distance from the shower axis is sensitive to the mass of the primary particle, so that mass identifiers like  $S^{100}$  or  $S^{200}$  combined with the muon information about EAS could be established and demonstrated to be useful [6] for the analysis of real data.

## 2. RADIAL DEPENDENCE OF THE CHARGED PARTICLE DENSITY

The general concept of the studies, as reported, in particular in ref.5 and 6 is the following:

A sample of CORSIKA simulated EAS initiated by protons and iron nuclei at various energies has been hitting the KASCADE-Grande array. Using GEANT code [14], the energy deposit per charged particle (muons and electrons) has been evaluated as a function of the distance from the shower axis. From the simulated energy deposits the particle number has been again reconstructed as they would be experimental signal. From the reconstructed number of charged particles, found for each detector station of Grande array [9], the reconstructed charged particles density  $S(r)$  in the normal plane to the shower axis has been deduced. The original CORSIKA number of charged particles hitting each detector was also recorded for sake of comparison and controlling the reconstruction efficiency. The charged particle distributions, (either the sampled CORSIKA distributions  $\rho_{\text{ch}}(r)$  or the reconstructed distribution  $S(r)$ ), have been adjusted to a Lateral Density Distribution Function (LDF) as proposed by Linsley [15]:

$$\rho_{\text{ch}}(r) \text{ or } S(r) = (N/R_0^2) C(\alpha, \eta) (R/R_0)^{-\alpha} (1 + r/R_0)^{-(\eta-\alpha)},$$

where:  $C = \Gamma(\eta - \alpha)[2\pi\Gamma(2 - \alpha)\Gamma(\eta - 2)]^{-1}$  and  $\rho_{\text{ch}}(r)$  or  $S(r)$  – the particle density at a distance  $R$  from the shower core;  $N$  – the shower size (in our case  $N_{\text{ch}}$ , the total number of electrons and muons);  $R_0$  – Molière radius ( $R_0$  have been taken 92 m);  $r$  – radius (distance from the shower axis);  $\alpha, \eta$  – two shape parameters.

The total number of charged particles and the shape parameters  $\alpha$  and  $\eta$  are determined by the fit. Both cases, the charged particle density  $\rho_{\text{ch}}(r)$  provided by CORSIKA without taking into account the detector response and the reconstructed charged particle density  $S(r)$  have been investigated. In course of our studies the Linsley LDF has been proven to be most adequate, though for reasonable determination of the density, say  $S^{500}$  are shorter, fitting ranges around  $r = 500$  should be used. The Linsley LDF, resulting from a modification of the NKG function [16] remedies some problems with the NKG function at large distances.

It should be stressed that the present paper reports results from an analysis of event-by-event “data”, considering *single* showers in terms of Linsley’s LDF, with the aim to infer the fluctuations of  $S(r)$  and of the shape parameters  $\alpha, \eta$ .

The analysis takes use of the programs SHOWREC [17] and the extended version STATSHW [18] which have been developed for such studies. Actually these programs are devised to be used in the same way for the analysis of real

data observed by the KASCADE-Grande experiment. The reconstruction of real data implies various cuts for an acceptable reconstruction of the data, e.g. a condition for the shape parameters  $\alpha, \eta$ , which will select in an energy dependent way a sub-sample from the total sample of observed EAS. Therefore the distribution of quantities derived from the reconstructed shower sample is distorted and must be corrected by efficiency factors reflecting the survival of the applied cuts. This work, relevant for the analysis of real showers, is still in progress.

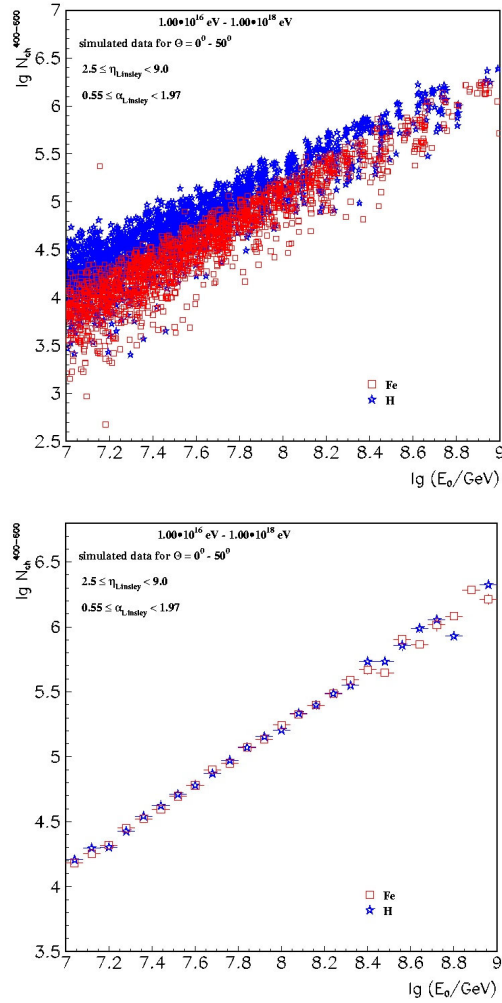


Fig. 1 – The energy variation of: a)  $\lg N_{\text{ch}}^{400-600}$  for EAS initiated by H and Fe; b)  $\lg N_{\text{ch}}^{400-600}$  for EAS initiated by H and Fe.

### 3. ENERGY ESTIMATION

In order to derive adequate observables from the lateral density distribution of charged EAS particles which may be used for an estimate of the primary energy, simulated files has been analyzed with STATSHW. A large set of showers produced by H, C and Fe primaries with the energies in 8 ranges from  $10^{16}$  eV to  $10^{18}$  eV have been simulated with CORSIKA version 6.023 [10] using the QGSJET model [19] for the hadronic interaction.

Our previous studies [4, 8] preferred for Grande experiment, instead of the value of a specific  $r$ , the charged particle density integrated in the range 400 – 600 m,  $N_{\text{ch}}^{400-600}$ .

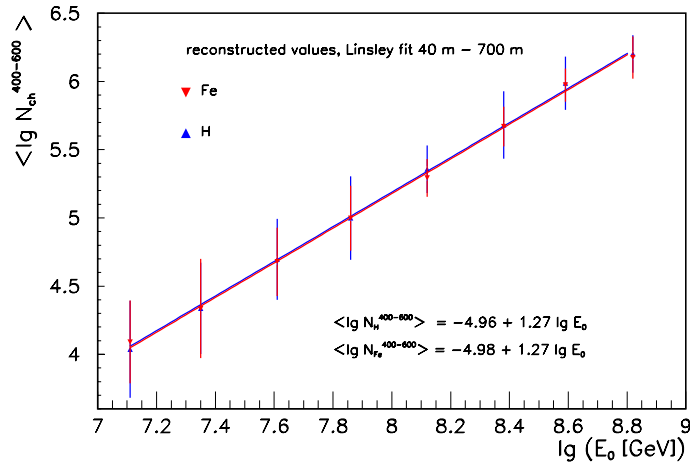


Fig. 2 – Quantification of the energy calibration by a linear relation.

Figure 1a shows the energy variation of  $\lg N_{\text{ch}}^{400-600}$  of all reconstructed showers initiated by H and Fe in the energy range  $(1.00 \cdot 10^{16} - 1.00 \cdot 10^{18})$  eV. Figure 1b shows the energy variation of the mean value of  $\lg N_{\text{ch}}^{400-600}$ . We observe a larger spread for H initiated showers, but the profile indicates the independence from the mass.

Figure 2 displays a linear relation of the mean  $\lg N_{\text{ch}}^{400-600}$  with  $\lg E_0$ , resulting in the relations:

- for H :  $\langle \lg N_{\text{ch}}^{400-600} \rangle = -4.39 \pm 1.20 \lg E_0$ ,
- for Fe:  $\langle \lg N_{\text{ch}}^{400-600} \rangle = -4.16 \pm 1.18 \lg E_0$ .

This quantifies the energy calibration and its independence from mass within the uncertainties, which are in fact considerable.

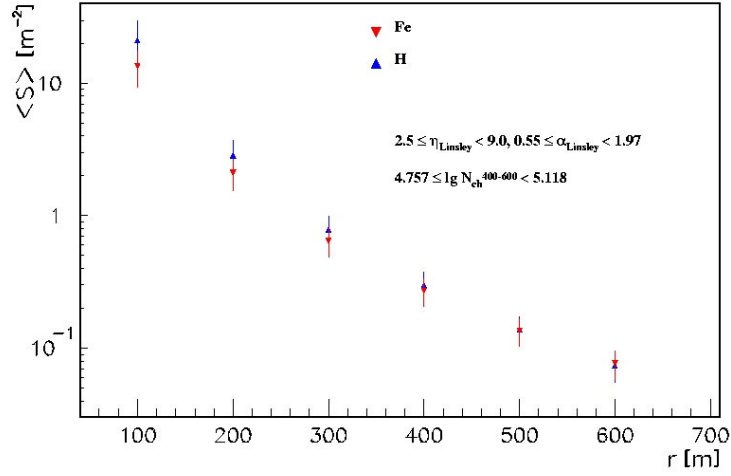


Fig. 3 – The mean radial lateral distribution for Fe and proton induced EAS for a particular  $\lg N_{\text{ch}}^{400-600}$  range, evaluated in a specific window of the shape parameters.

#### 4. MASS DISCRIMINATION

Figure 3 displays the mean lateral charged particle density distributions for the simulated H and Fe showers in a certain  $\lg N_{\text{ch}}^{400-600}$  range, indicating: a differences between primaries of different at distances closer to the shower core (100 m – 200 m), while at 500 m – 600 m the they tend to be identical.

It should be noted that first comparisons of the simulations lateral distributions with those extracted from the KASCADE-Grande data show a promising agreement [8]. This work is in progress.

Our previous work [3, 4, 5, 6] has already indicated that the charged particle density  $S(r)$  at smaller radial range  $r = 100 - 200$  and correlated with the integrated muon density  $N_{\mu}^{40-700}$  (muon size) exhibits features for mass discrimination.

Figure 4 shows the distributions of  $\lg N_{\text{ch}}^{100-200}$  for the simulated for H and Fe showers for different bins of  $\lg N_{\text{ch}}^{400-600}$ , corresponding to energy intervals used in a previous communication of KASCADE-Grande data [20]. With increasing  $\lg N_{\text{ch}}^{400-600}$ , corresponding to increasing EAS energies, we notice an increased discrimination between H and Fe showers. The discriminative features appear more pronounced by the correlation of  $\lg N_{\text{ch}}^{100-200}$  with the muon shower size. This is shown in Fig. 5 in a scatter plot of the event-by-event correlation for selected ranges of  $\lg N_{\text{ch}}^{400-600}$  (corresponding to different incident

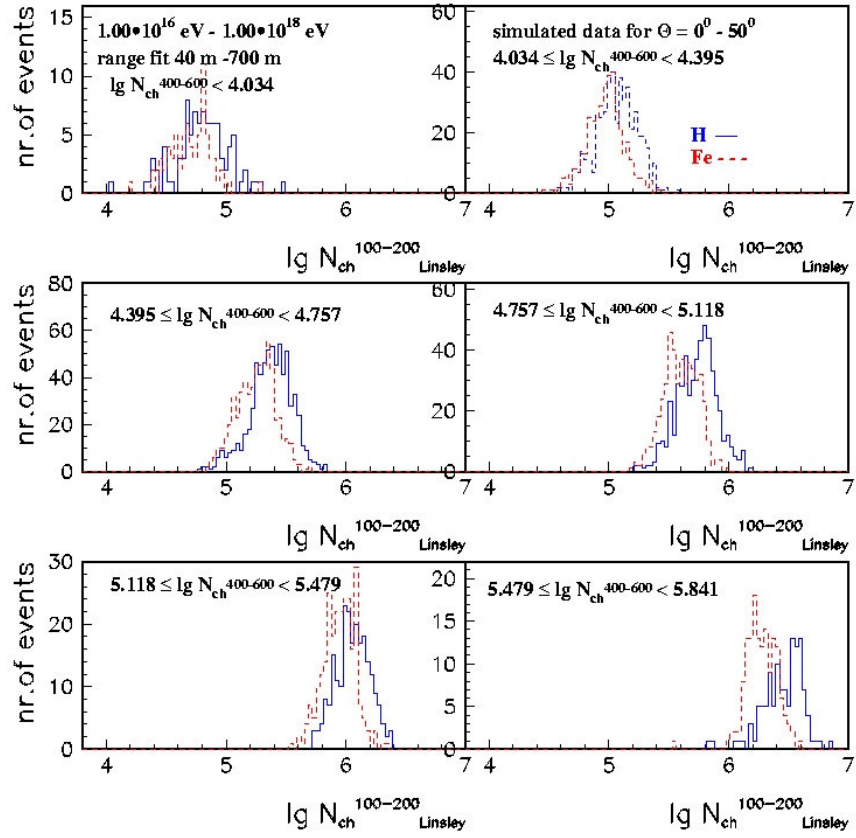


Fig. 4 – Distributions of  $\lg N_{\text{ch}}^{100-200}$  for different  $\lg N_{\text{ch}}^{400-600}$  bins.

energy ranges) exhibiting promising features for the discrimination of primary mass discrimination.

## 5. NONPARAMETRIC STATISTICAL ANALYSIS

For a quantification of the qualitative features evidenced by the plots given above, a multidimensional statistical analysis could be applied with a quantitative estimation of the discriminative power of different correlations between the EAS observables [21]. Such technique has been used for the present cases in our previous papers [4, 6], where based on ANI code [22] the discrimination of 3 classes of EAS primaries, H, C, and Fe has been represented by the degree of separation of multidimensional distributions. The procedure takes

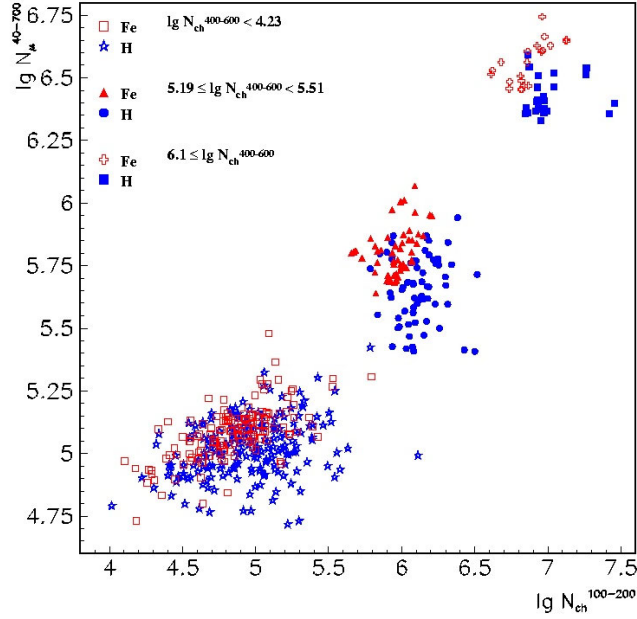


Fig. 5 – Correlation of  $\lg N_{\text{ch}}^{100-200}$  with the muon shower size  $N_{\mu}^{40-700}$ .

into account the EAS fluctuations and specifies the uncertainties by estimating the true classification and misclassification probabilities. The classification is based on the Bayesian decision rules. Using such technique, the lateral distribution of the charged EAS particles represented by adequately defined observables, shows evidence for quantitatively expressed mass discrimination.

Figure 6a displays the results for the true-classification and miss-classification probabilities for sets of observables found relevant for the mass discrimination.

Figure 6b displays the results for the true-classification for each cosmic primary H, C and Fe for the energy range of interest for the KASCADE-Grande experiment. It indicates an improved classification with an increasing energy range and increasing primary mass.

## 6. CONCLUDING REMARKS

The reconstruction of the charged particle density distribution from quasi-experimental data has been performed in an event-by-event mode, by use of the Linsley LDF. The procedure adjusts the Linsley LDF in the radial ranges 40 – 700 m and controls the fitting procedure by restricting the shape parameters in a particular window  $0.55 < \alpha < 1.97$ ,  $2.5 < \eta < 9.0$ . It should be

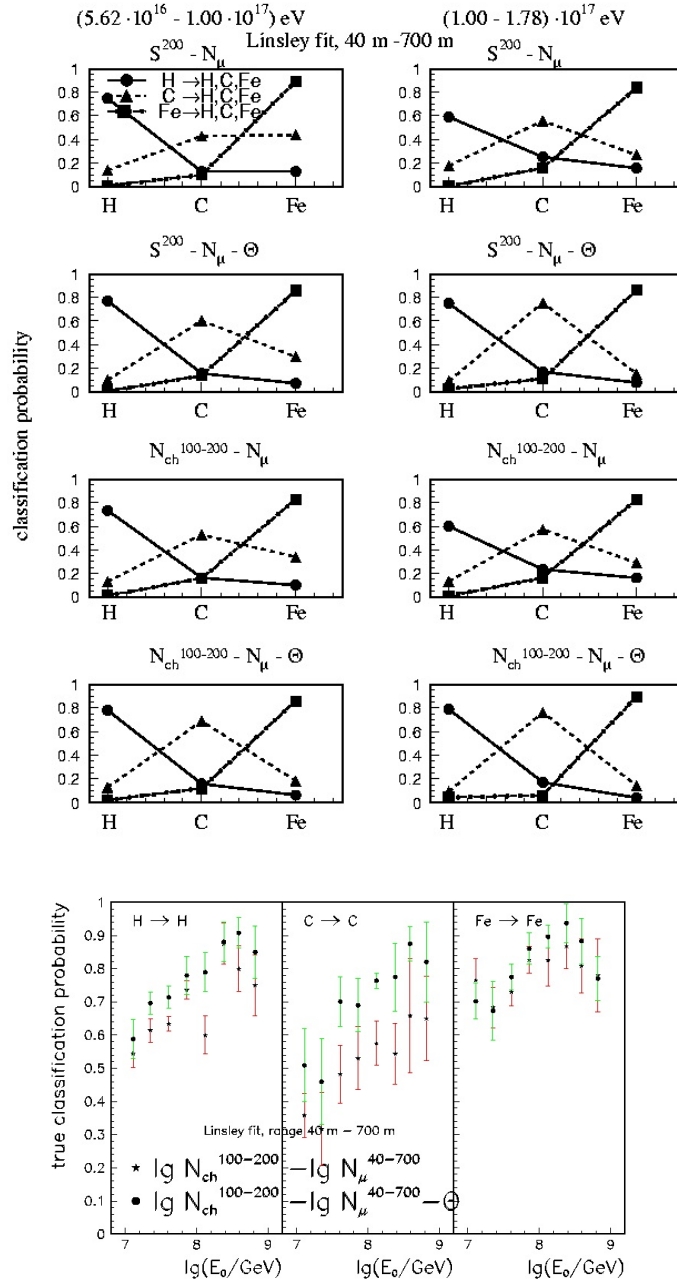


Fig. 6 – a) True-classification and miss-classification probabilities for sets of observables found relevant for the mass discrimination; b) true-classification for each cosmic primary H, C and Fe for the energy range of interest for the KASCADE-Grande experiment.

noted that in a similar analysis the AGASA collaboration [23] did fit only the  $\eta$  parameter and kept  $\alpha \approx 1.2$  constant.

Summarizing it may be remarked:

a) The EAS charged particle density as reconstructed from quasi-experimental data is sensitive to the energy of the primary particle in the range of distances of 500 m – 600m, with a relation nearly independent from the primary mass. Observables like  $S^{500}$ ,  $S^{600}$ , and  $\lg N_{\text{ch}}^{400-600}$  can be defined as energy estimator for the primary energy,

b) The reconstructed charged particle density at smaller distances (100 m – 200 m) from the shower axis exhibits features for the mass discrimination. the correlations of observables  $\lg N_{\mu}^{40-700} - \lg N_{\text{ch}}^{100-200}$  are suggested to be relevant in KASCADE-Grande experiment,

c) The features can be quantified by applying non-parametric statistical techniques for the analysis of multivariate distributions.

*Acknowledgements.* I would like to thank Prof. Dr. H. Blümer for the kind hospitality in Forschungszentrum Karlsruhe and all the KASCADE-Grande collaboration for fruitful discussions during different research visits. I am grateful to Prof. Dr. H. Rebel and Dr. A. Haungs for continous help and suggestions in pursuing these studies, which have been financially supported by the Romanian Ministry CEEEX 05-D11-79/2005 project. Special thanks are going to Prof. Dr. O. Sima for developing SHOWREC and STATSHW programs. The help of Dr. A. F. Badea, DP. B. Mitrica and DP G. Toma in elaborating the algorithms for calculating the reconstructed charge particle densities and of DM J. Oehlschläger in preparing the CORSIKA simulations is gratefully acknowledged. I am grateful to DM M. Duma for technical assistance and to Dr. K. Bekk for prompt help in different computer problems.

## REFERENCES

1. I.M. Brancus *et al.*, J. Phys. G: Nucl. Part. Phys., **29**, 453 (2003).
2. B. Mitrica *et al.*, Interner Bericht KASCADE-Grande, 2003-03.
3. I.M. Brancus *et al.*, Interner Bericht KASCADE-Grande, 2004-02.
4. I.M. Brancus *et al.*, Interner Bericht KASCADE-Grande, 2005-02.
5. H. Rebel, O. Sima *et al.*, KASCADE-Grande collaboration, *Proc. International Cosmic Rays Conference*, August 3-10, 2005, Pune, India, vol. 6, p. 297.
6. I.M. Brancus *et al.*, KASCADE-Grande collaboration, *Proc. International Cosmic Rays Conference*, August 3-10, 2005, Pune, India, vol. 6, p. 361.
7. G. Toma *et al.*, *Proc. 26-th European Cosmic Rays Symposium*, September 5-8, 2006, Lisbon, Portugal.
8. I.M. Brancus *et al.*, Interner Bericht KASCADE-Grande, 2007-01.
9. A. Haungs *et al.*, KASCADE-Grande collaboration, *Proc. International Cosmic Rays Conference*, August 2003, Tsukuba, Japan, vol. 2, p. 895.
10. D. Heck *et al.*, Report FZKA-Report 6019, Forschungszentrum Karlsruhe, 1988.
11. A.M. Hillas *et al.*, Proc. 12-th ICRC, 1971.

12. H.Y. Dai *et al.*, *J. Phys. G Nucl. Phys.*, **14**, 793 (1998).
13. M. Nagano *et al.*, *Astropart. Phys.*, **13**, 277 (2000).
14. \* \* \*, *GEANT user's guide*, CERN program library, W5013, 1993.
15. J. Linsley *et al.*, *Journ. Phys. Soc. Japan*, **17**, A-III (1962).
16. K. Greisen, *Ann. Rev. Nucl. Sci.* **10**, 63 (1960).
17. O. Sima *et al.*, Report FZKA 6985, Forschungszentrum Karlsruhe, 2004.
18. O. Sima *et al.*, Interner Bericht KASCADE-Grande, 2005-01.
19. N.N. Kalmykov and S.S. Ostapchenko, *Phys. At. Nucl.*, **56**, 346 (1993).
20. R. Glastetter *et al.*, KASCADE-Grande collaboration, *Proc. International Cosmic Rays Conference*, August 3-10, 2005, Pune, India, vol. 6, p. 101.
21. A.A. Chilingarian, *Comp. Phys. Commun.*, **54**, 381 (1989); A.A. Chilingarian *et al.*, *Nuovo Cim.*, **14**, 355 (1991).
22. \* \* \*, ANI reference manual, 1999, unpublished.
23. M. Teshima, private communication.